Proceedings of the 9th International Symposium on
Dynamics and Control of Process Systems (DYCOPS 2010),
Leuven, Belgium, July 5-7, 2010
Mayuresh Kothare, Moses Tade, Alain Vande Wouwer, Ilse Smets (Eds.)

Modelling lipid production in microalgae

Francis Mairet * **Olivier Bernard** * **Pierre Masci** *
Thomas Lacour ** **Antoine Sciandra** **

* *COMORE-INRIA, BP93, 06902 Sophia-Antipolis Cedex, France (e-mail: olivier.bernard@inria.fr).*
** *LOV, UMR 7093, BP28, 06234 Villefranche-sur-mer, France*

Abstract: Microalgae offer potentially great opportunities for producing biofuel. In order to optimize triglycerid production, this article proposes a dynamical model of microalgal lipid production. In this model, intracellular carbon is divided between a functional pool and two storage pools (sugars and neutral lipids). The various intracellular carbon flows between these pools lead to a complex dynamic with a strong discrepancy between accumulation and mobilization of neutral lipids. This generates an hysteresis which has been observed experimentally. The model has been validated with experiments of *Isochrysis affinis galbana* (T. iso) culture under various nitrogen limitation conditions.

Keywords: phytoplankton, growth model, nitrogen starvation, neutral lipid, biofuel

1. INTRODUCTION

Various photosynthetic microorganisms (microalgae or cyanobacteria) have shown an ability to synthesize and accumulate considerable amounts of lipids [Chisti 2007]. Indeed, the photosynthetic yield of these microorganisms (abusively gathered under the name "microalgae") is higher than for terrestrial plants. Its leads to algal biomass productivities of several tens of dry biomass tons per hectare and per year [Huntley and Redalje 2007]. When combined with a high neutral lipid content [Metting 1996], microalgae can potentially produce biofuel in a range of magnitude higher than for terrestrial plants. This potential has led some authors to consider that microalgae could be one of the main biofuel producers in the future [Huntley and Redalje 2007, Chisti 2007].

However, lipid production in microalgae is not straightforward and suffers from many limitations [Pulz 2001, Carvalho et al. 2006]. For example, a nitrogen starvation increases the cell lipid content but it also strongly affects the growth rate. The lipid productivity, which is the consequence of these two factors, needs a trade off between biomass production and oil content.

The main objective of this work is to propose a model for lipid production under nitrogen stress which will guide the research of an optimisation strategy. The model must thus find a trade off between realism, in order to accurately represent the key variables of the process, and simplicity so that it can be mathematically tractable and suitable to solve optimal control problems. The simplest model for describing growth of a population of microalgae limited by a nutrient (*e.g.* nitrogen or phosphorus) is the Droop model [Droop 1968, 1983]. This models assumes that the growth rate depends on the internal concentration of the limiting element. More accurate models have been proposed to deal with the coupling between nitrogen and carbon assimilation in various light conditions [Geider et al. 1998, Faugeras et al. 2004, Pahlow 2005]. However none of these models predicted the lipid concentration and, to our knowledge, the model which is presented in this work is the first dealing with neutral lipid production by microalgae. The main objective of this dynamical model is to identify conditions that optimise the lipid synthesis.

The article is structured as follows: after a material and methods section, the model assumptions are detailled and then the resulting model equations are presented. Then, we describe the calibration procedure and we compare the model with experimental data of a *Isochrysis affinis galbana* culture, with various nitrogen limitations. Finally, a section is devoted to the analysis of the model behavior.

2. MATERIAL AND METHODS

2.1 Culturing device

Cultures of *Isochrysis affinis galbana*, (clone T-iso) were grown in 5 L cylindrical vessels at constant temperature ($22.5°C$), light ($430 \pm 30\,\mu mol\,quanta.m^{-2}.s^{-1}$ in the centre of the culture vessel) and pH (maintained at 8.0 by automatic injection of CO_2). The experiment consists in imposing various nitrogen limitations through a succession of dilution rates changes followed by transient periods to reach the equilibrium. Finally, dilution was stopped to obtain a nitrogen starvation. Variations of the influent nitrogen concentration were used to maintain biomass concentration in an appropriate range. Figure 1 presents the operating conditions.

2.2 Measurements

The following measurements were performed: nitrate concentrations (Technicon Auto-analyser), biovolumes (optical particle counter Hiac/Royco), concentrations of particulate carbon and nitrogen (CHN analyser, PerkinElmer), total carbohydrates concentrations (by the phenol method), and neutral lipid (quantitative extraction and separation

with column chromatography on silica gel, Extract-Clean, Alltech). Carbohydrates and neutral lipid measurements are converted in $g[C]$ using standard values of conversion. For more details on the experiment protocol see Le Floc'h et al. [2002].

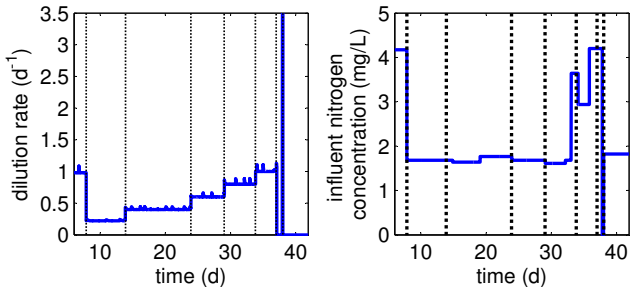

Fig. 1. Operating conditions for experiment with T-iso. Dilution rate variations impose various nitrogen limitations.

3. MODEL DESIGN

3.1 Variables and reaction network

Our objective is to propose a simple model which can support a control approach and an optimisation algorithm. It must therefore keep a level of minimal complexity to be mathematically tractable. We therefore limited the number of variables to the most important ones. We focus on the growth of microalgae, whose biomass, in terms of organic carbon, is denoted x. These microalgae are limited by an inorganic nitrogen source (nitrate, denoted s). In line with Ross and Geider [2009], we consider that organic carbon can be split into functional and storage pools. The functional compartment (f) includes the biosynthetic apparatus (proteins and nucleic acids) and the structural material (membranes mainly made of glycolipids and phospholipids). Contrarily to Ross and Geider [2009], we add a new distinction: the storage pool is divided into a sugar reserve compartment (g) and a neutral lipid reserve compartment (l).

Nutrient uptake and biomass growth are known to be uncoupled processes for microalgae [Droop 1983, Geider et al. 1998] leading thus to variations in the internal quota of nutrient.

Nutrient is taken up by the microalgae to make cellular nitrogen (n) at rate $\rho(s)$. This flux of nitrogen can be summarized in the following macroscopic reaction which represents the mass flux between the inorganic and organic compounds:

$$s \xrightarrow{\rho(s)x} n \tag{1}$$

The absorption rate $\rho(s)$ is taken as a Michaelis-Menten function:

$$\rho(s) = \rho_m \frac{s}{s + K_s} \tag{2}$$

with K_s the half-saturation constant for the substrate and ρ_m the maximum uptake rate.

In line with the Droop model philosophy, we consider that the specific growth rate μ, *i.e.* the net incorporation of CO_2 is an increasing function of the internal quota of nutrient ($q_n = \frac{n}{x}$). We assume that inorganic carbon is first incorporated in the pool of sugars g:

$$CO_2 \xrightarrow{\mu(q_n)x} g \tag{3}$$

This macroscopic reaction summarizes the set of reactions that occur in the dark phase of photosynthesis, and that lead, through the Calvin cycle to the production of carbohydrates such as glucose 6-phosphate. The mathematical expression for the specific growth rate μ is chosen using Droop model:

$$\mu(q_n) = \bar{\mu}(1 - \frac{Q_0}{q_n}) \tag{4}$$

where $\bar{\mu}$ and Q_0 represent the theoretical maximum growth rate and the minimum nitrogen quota allowing growth, respectively.

The sugar compartment g is then used in a second stage to synthesize the functional elements of the biomass f:

$$g \xrightarrow{\alpha\rho(s)x} f \tag{5}$$

This reaction corresponds mainly to the synthesis of proteins and nucleic acids, which depends on nitrogen availability. We therefore consider as in Ross and Geider [2009] that the synthesis rate is proportional to the nitrogen assimilation rate.

The sugar compartment g is also used in a parallel pathway to synthesize neutral lipid (*i.e.* mainly triglycerids):

$$g \xrightarrow{\beta q_n \mu(q_n)x} l \tag{6}$$

We assume that this rate of lipid synthesis depends on the photosynthesis rate $\mu(q_n)$, but that it is modulated by the nitrogen quota. This assumption is based on the work of Sukenik and Livne [1991] who have observed the dependence of lipid production on the growth rate in T-iso cultures.

These neutral lipids are then mobilized to the production of functional carbon (mainly membranes):

$$l \xrightarrow{\gamma\rho(s)x} f \tag{7}$$

The rate of this reaction is assumed to be proportional to the synthesis of proteins and nucleic acids (reaction 5).

A representation of the carbon flows is given on Fig.2. Note that it is a rather strong simplification of the complex metabolism of the cell. Thus, reaction 6 can be decomposed in two steps with the formation of fatty acids as intermediate. These fatty acids can be used directly to synthetize structure (reaction 7). As "free" fatty acids are not stored in the cell [Ohlrogge and Browse 1995, Guschina and Harwood 2009], neutral lipids are used to store or to provide fatty acids when there is a disequilibrium between fatty acid synthesis and consumption [Thompson-Jr 1996]. Nevertheless, as fatty acid pool is of negligible size, we do not represent its dynamic in order to keep a low level of model complexity.

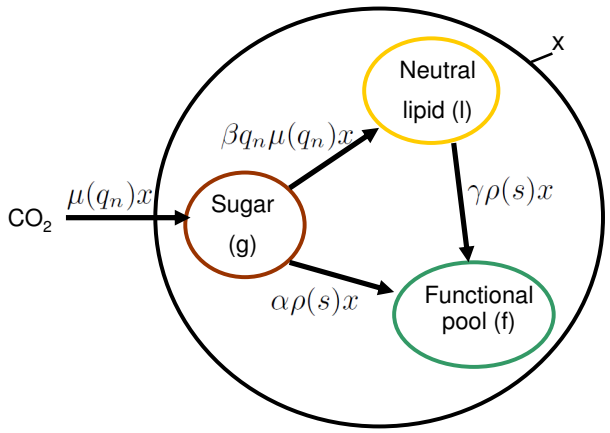

Fig. 2. Representation of the carbon flows. The dynamic of neutral lipids results from the unbalance between lipid synthesis and mobilization.

3.2 Model equations

Assuming that the main mass transfer of carbon and nitrogen can be summarized by the reactions (1) to (7), the time-varying evolution equations resulting from mass balances considerations [Bastin and Dochain 1990] in a homogeneous photobioreactor are given by:

$$\begin{cases} \dot{s} = Ds_{in} - \rho(s)x - Ds \\ \dot{n} = \rho(s)x - Dn \\ \dot{g} = (1 - \beta q_n)\mu(q_n)x - \alpha\rho(s)x - Dg \\ \dot{l} = \beta q_n \mu(q_n)x - \gamma\rho(s)x - Dl \\ \dot{f} = (\alpha + \gamma)\rho(s)x - Df \end{cases} \tag{8}$$

Where D is the dilution rate (ratio of the influent flow rate over the photobioreactor volume) and s_{in} the influent nitrate concentration.

From equations (8), we can deduce the dynamics of the nitrogen quota q_n, the carbon biomass $x = f + g + l$, and the fractions of neutral lipid $q_l = l/x$ and functional carbon $q_f = f/x$, leading to the following set of equations:

$$\begin{cases} \dot{s} = Ds_{in} - \rho(s)x - Ds \\ \dot{q_n} = \rho(s) - \mu(q_n)q_n \\ \dot{x} = \mu(q_n)x - Dx \\ \dot{q_l} = (\beta q_n - q_l)\mu(q_n) - \gamma\rho(s) \\ \dot{q_f} = -q_f\mu(q_n) + (\alpha + \gamma)\rho(s) \end{cases} \tag{9}$$

It is worth noting that the first 3 equations of system (9) are exactly the Droop model [Droop 1968, 1983]. This model presents the advantage of being simple and having been extensively validated [Droop 1983, Sciandra and Ramani 1994, Bernard and Gouzé 1999]. The system has a cascade structure: the dynamics of the fractions q_l and q_f do not influence the kinetics of the biomass.

4. MODEL CALIBRATION

4.1 Parameter value computation

First, we present some model properties that will be used to identify the parameter values. In the Droop model, it can be proved (see Bernard and Gouzé [1995]) that the nitrogen quota stays between two bounds:

$$Q_0 \leq q_n \leq Q_m \tag{10}$$

with

$$Q_m = Q_0 + \frac{\rho_m}{\bar{\mu}} \tag{11}$$

Q_m represents the maximum cell quota obtained in conditions of non limiting nutrients, and the minimum quota, Q_0, is obtained in batch conditions after limiting nutrient depletion. Thus, we can deduce a maximal growth rate μ_m:

$$\mu_m = \mu(Q_m) = \bar{\mu}(1 - \frac{Q_0}{Q_m}) \tag{12}$$

This property will be used to compute $\bar{\mu}$, from the minimal and maximal nitrogen quota Q_0 and Q_m:

$$\bar{\mu} = \mu_m \frac{Q_m}{Q_m - Q_0} \tag{13}$$

In order to compute steady states for the fractions of neutral lipid q_l^* and functional carbon q_f^*, the dynamics of q_l and q_f in (9) can be rewritten:

$$\begin{cases} \dot{q_l} = [(\beta - \gamma)q_n - q_l]\,\mu(q_n) - \gamma\dot{q_n} \\ \dot{q_f} = [(\alpha + \gamma)q_n - q_f]\,\mu(q_n) + (\alpha + \gamma)\dot{q_n} \end{cases} \tag{14}$$

At steady state, as $\dot{q_n} = 0$, we obtain the following equilibrium:

$$\begin{cases} q_l^* = (\beta - \gamma){q_n}^* \\ q_f^* = (\alpha + \gamma){q_n}^* \end{cases} \tag{15}$$

The model predicts thus, at steady state, that neutral lipid and functional carbon quotas are proportional to the nitrogen quota. Steady state of the sugar fraction q_g^* is deduced from the relation $q_l + q_f + q_g = 1$:

$$q_g^* = 1 - (\beta + \alpha){q_n}^* \tag{16}$$

As both $q_l^*(q_n)$ and $q_f^*(q_n)$ are linear increasing functions, $q_g^*(q_n)$ is a linear decreasing function.

Parameters α, β and γ can then be computed from the previous equations, using measurements obtained at equilibrium.

4.2 Parameter estimation

We uncouple the estimation into two groups of parameters: the Droop parameters (Q_0, $\bar{\mu}$, ρ_m, K_s) and the intracellular carbon flow parameters (α, β, and γ). The

Droop parameters can be easily determined, on the basis of dedicated experimental conditions, and then, the carbon parameters are identified using steady state observations.

The minimal nitrogen quota Q_0 is obtained from the nitrogen quota measurement during nitrate starvation (at the end of the experiment). The maximum nitrogen quota Q_m and specific growth rate μ_m are estimated directly from the nitrogen quota measurements and the dilution rate during the non-limited growth phase at the beginning of the experiment (before the first dilution rate change, see Fig. 3). The maximal absorption rate ρ_m and growth parameter $\bar{\mu}$ are obtained with relations (11) and (13). The half-saturation constant $K_s = 0.018\, mg[N]/L$ is taken from previous experiments (data not shown).

The second step of the calibration procedure concerns the intracellular carbon flow parameters. The data obtained at steady state for the several dilution rates are used to determine, thanks to equations (15), the parameters α, β, and γ. Using an estimation of the slopes of $q_l^*(q_n)$ and $q_f^*(q_n)$ lines, we obtain a system of two equations with three unknown parameters. We have therefore one freedom degree to fit the transient behavior of the model to the data using a minimization algorithm.

The results of the calibration are given in table 1.

Table 1. Parameters obtained by the calibration of the model

Parameter	Value
Minimal nitrogen quota Q_0	0.05 $mg[N].mg[C]^{-1}$
Maximal nitrogen quota Q_m	0.11 $mg[N].mg[C]^{-1}$
Maximal growth rate μ_m	1 d^{-1}
Protein synthesis coefficient α	3.1 $mg[C].mg[N]^{-1}$
Fatty acid synthesis coefficient β	3.5 $mg[C].mg[N]^{-1}$
Fatty acid mobilisation coefficient γ	1.7 $mg[C].mg[N]^{-1}$
Half-saturation constant K_s	0.018 $mg[N].L^{-1}$
Theoretical maximum growth rate $\bar{\mu}$†	1.83 d^{-1}
Maximal uptake rate ρ_m†	0.11 $mg[N].mg[C]^{-1}.d^{-1}$

† : Parameters computed from Q_0, Q_m and μ_m

5. SIMULATION AND COMPARISON WITH EXPERIMENTAL DATA

Continuous cultures of *Isochrysis affinis* T-iso are used in order to assess the ability of the model to reproduce experimental data. Results shown in Fig. 3 demonstrate that the model reproduces quite accurately the dynamics of s, q_n and x. This corroborates the fact that the Droop model has been widely validated [Droop 1983, Sciandra and Ramani 1994, Bernard and Gouzé 1999] for its aptitude to predict both biomass and remaining inorganic nitrogen. The simulated distribution of intracellular carbon between sugars, neutral lipids and functional pool also accurately follows the experimental data (Fig. 4).

6. ANALYSIS OF THE MODEL BEHAVIOR

In this section, we analyse the behavior of the model compared with the experimental data in order to explain the complex dynamics of neutral lipid quota.

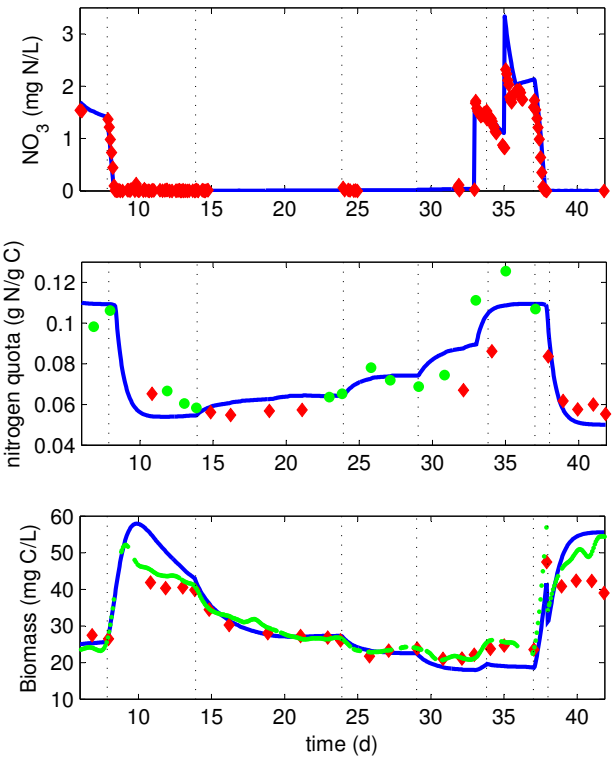

Fig. 3. Comparison of the Droop model (blue lines) with the data of T-iso culture under various nitrogen conditions. Nitrogen quota is directly measured (red diamond) or estimated from nitrogen balance (green circle). Carbon biomass is measured (red diamond) and deduced from biovolume measurements (green circle). Vertical lines indicate dilution rate changes.

6.1 Steady state

Equation (15) shows that the neutral lipid quota is proportional to the nitrogen quota in stabilized culture. This result is validated with the experimental data obtained at steady states in chemostats run at various dilution rates (see Fig. 5).

6.2 Hysteresis behaviour

Let us consider a situation where the cells are in a steady state characterized by a high nitrogen content q_{n1}^*. If the dilution rate is decreased, the cells undergo a decrease of their nitrogen quota down to a value $q_{n2}^* < q_{n1}^*$. This means that, during this transient, we have $\dot{q_n} < 0$ [Bernard and Gouzé 1995]. Using equation of $\dot{q}_l$ in (14), the dynamic of $z = q_l - (\beta - \gamma)q_n$ is:

$$\dot{z} = -z\mu(q_n) - \beta\dot{q_n} \tag{17}$$

As z is initially null, z remains non-negative during this transient so that q_l is above the line of equation $q_l = (\beta - \gamma)q_n$, which is indeed the steady state line. Once the nitrogen quota has reached its steady state value, we have $\dot{q_n} = 0$. It follows that z tends toward zero and q_l finally reaches its steady state on the line $q_l^* = (\beta - \gamma){q_n}^*$.

Note that this behaviour is possible only since $\mu(q_n)$ is not zero, and is decreasing from $\mu(q_{n1})$ down to $\mu(q_{n2}) > 0$.

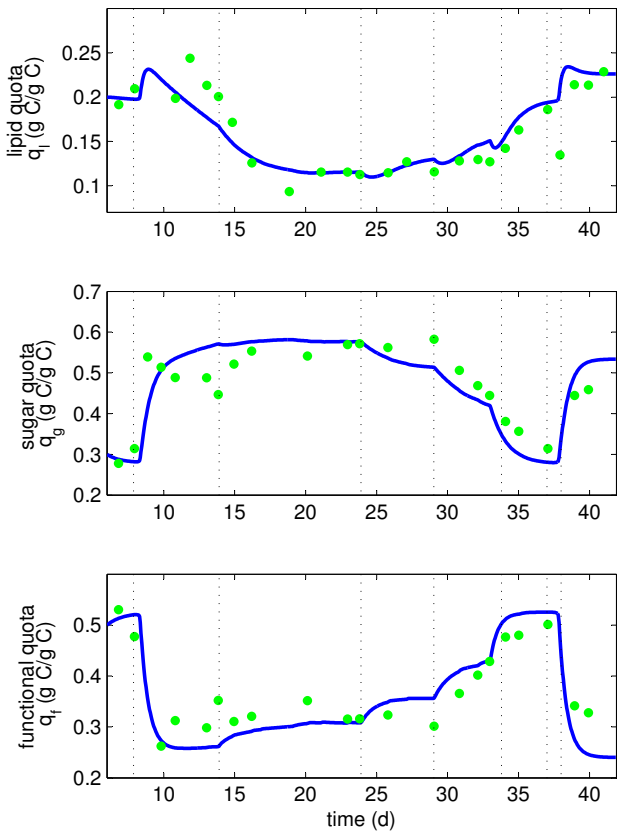

Fig. 4. Comparison of the lipid model with the data of *Isochrysis affinis* T-iso culture under various nitrogen limitation rates. Evolution of the intracellular carbon quotas. Vertical lines indicate dilution rate changes.

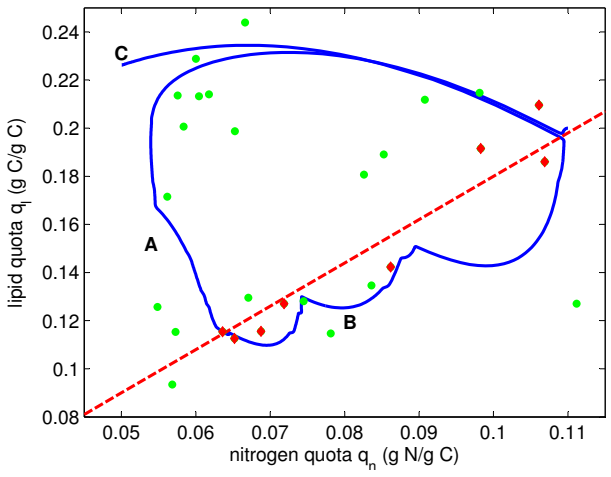

Fig. 5. The dependence of neutral lipid quota q_l on nitrogen quota q_n. Red diamond: steady state data, red dashed line: model equilibrium. A: decrease of q_n, B: increase of q_n, C: decrease of q_n until growth stops (nitrogen starvation).

This transient behaviour of q_l is observed on Fig.4: the neutral lipid mobilisation decreases faster than its synthesis which explains transient increase of the neutral lipid quota.

The same reasoning can explain the behaviour of the lipid content, when the internal nitrogen quota is increased (following for example an increase in the dilution rate). In this case, we can show that q_l will increase under the line $q_l = (\beta - \gamma)q_n$. This behavior leads to a phenomenon of hysteresis experimentally observed: the trajectory between two steady states for an increase in nitrogen limitation is very different from the one of a decrease in nitrogen limitation (see Fig. 5).

6.3 Nitrogen starvation

In a case of nitrogen starvation (*i.e.* $s = 0$), the steady state value of q_l can be computed, when q_n decreases from Q_m down to Q_0 as follows (see Appendix for details):

$$q_l^\dagger = Q_0 \left[(\beta - \gamma) + \beta \ln \left(\frac{Q_m}{Q_0} \right) \right] \tag{18}$$

If the parametric condition $\frac{\beta-\gamma}{\beta} < \frac{Q_0}{Q_m - Q_0} \ln \left(\frac{Q_m}{Q_0} \right)$ is verified, this expression shows that the final lipid content after exhaustion of the nitrate is greater than $(\beta - \gamma)Q_m$, the maximum amount of lipid reached in balanced growth. With the computed parameters (Table 1), this condition is fulfilled. Nevertheless, it may be species dependent, meaning that for some species balanced growth may allow to reach higher lipid quota.
Nitrogen starvation at the end of the experiment confirms this result. A comparison between the nitrogen limitation (starting at day 5) and the nitrogen starvation (starting at day 38) is of particular interest. The model predicts that such a protocol should lead to radically different behaviour of neutral lipid quota. In the nitrogen limitation, a lower value of the lipid content should be reached after a transient increase, while the starvation should lead to an enhanced value of q_l, higher than the maximum obtained in balanced growth conditions. On the other side, the sugar quota should increase in both situations. Fig. 4 and 5 show that these predictions are experimentally verified.

6.4 Consequences on neutral lipid productivity

This study emphasises that neutral lipid content at equilibrium is proportional to nitrogen quota. Therefore, it is worth noting that a continuous culture at low nitrogen quota leads to both a low growth rate and a low lipid content, and thus a weak productivity. However, a transient increase of lipid content is obtained when the nitrogen quota decreases (*i.e.* when there is a disequilibrium between carbon and nitrogen flows).
Finally, this study highlights the fact that the highest values of the neutral lipid content can be obtained in two very different modes. Either after a nitrogen starvation, or at maximum growth rate in non limiting conditions for a continuous culture. This provides an hint to identify the optimal productivity conditions, which are probably a species dependent combination of these two working modes. The model simplicity will be the key point to make the optimisation study tractable from a mathematical point of view.

7. CONCLUSIONS

We have proposed a model for neutral lipid production by microalgae. The strength of this model is to describe accurately both the steady state and the transient phases. The model catches the different dynamics encountered in various physiological conditions from low nitrogen limitation to starvation. The model, based on Droop approach, has a minimal degree of complexity so that it can be mathematically analysed. It highlights and explains the phenomenon of hysteresis in neutral lipid production which has been experimentally verified.

The model must be assessed and validated with other microalgal species. It will then be used to predict and optimize neutral lipid production in the perspective of large scale biofuel production. It may also endorse a model based closed loop control in order to on-line implement the optimal strategy [Mailleret et al. 2005].

ACKNOWLEDGEMENTS

This paper presents research results supported by the ANR-06-BIOE-014 Shamash project.

REFERENCES

Bastin, G. and Dochain, D. (1990). *On-line estimation and adaptive control of bioreactors*. Elsevier, New York.

Bernard, O. and Gouzé, J.L. (1995). Transient Behavior of Biological Loop Models, with Application to the Droop Model. *Mathematical Biosciences*, 127(1), 19–43.

Bernard, O. and Gouzé, J.L. (1999). Nonlinear qualitative signal processing for biological systems: application to the algal growth in bioreactors. *Math. Biosciences*, 157, 357–372.

Carvalho, A., Meireles, L., and Malcata, F. (2006). Microalgal reactors: A review of enclosed system designs and performances. *Biotechnol Prog*, 22(6), 1490–1506.

Chisti, Y. (2007). Biodiesel from microalgae. *Biotechnology Advances*, 25, 294–306.

Droop, M.R. (1968). Vitamin B12 and marine ecology. IV. the kinetics of uptake growth and inhibition in *Monochrysis lutheri*. *J. Mar. Biol. Assoc.*, 48(3), 689–733.

Droop, M.R. (1983). 25 years of algal growth kinetics, a personal view. *Botanica marina*, 16, 99–112.

Faugeras, B., Bernard, O., Sciandra, A., and Levy, M. (2004). A mechanistic modelling and data assimilation approach to estimate the carbon/chlorophyll and carbon/nitrogen ratios in a coupled hydrodynamical-biological model. *Nonlinear Processes in Geophysics* , 11, 515–533.

Geider, R., MacIntyre, H., and Kana, T. (1998). A dynamic regulatory model of phytoplanktonic acclimation to light, nutrients, and temperature. *Limnol Oceanogr*, 43, 679–694.

Guschina, I. and Harwood, J. (2009). *Algal Lipids and Effect of the Environment on their Biochemistry*. Springer New York.

Huntley, M. and Redalje, D. (2007). CO_2 Mitigation et Renewable Oil from Photosynthetic Microbes: A New Appraisal. *Mitigation et Adaptation Strategies for Global Change*, 12, 573 – 608.

Le Floc'h, E., Malara, G., and Sciandra, A. (2002). An automatic device for in vivo absorption spectra acquisition in phytoplanktonic cultures: application to the study of photoadaptation to light and nutrient variations. *J. Applied Phycol.*, 14, 435–444.

Mailleret, L., Gouzé, J.L., and Bernard, O. (2005). Nonlinear control for algae growth models in the chemostat. *Bioprocess and Biosystem Engineering*, 27, 319–328.

Metting, F. (1996). Biodiversity and application of microalgae. *Journal of Industrial Microbiology & Biotechnology*, 17, 477 – 489.

Ohlrogge, J. and Browse, J. (1995). Lipid biosynthesis. *The Plant Cell*, 7, 957–9708.

Pahlow, M. (2005). Linking chlorophyllnutrient dynamics to the Redfield N:C ratio with a model of optimal phytoplankton growth. *Mar Ecol Prog Ser*, 287, 33–43.

Pulz, O. (2001). Photobioreactors: production systems for phototrophic microorganisms. *Applied Microbiology et Biotechnology*, 57, 287–293.

Ross, O. and Geider, R. (2009). New cell-based model of photosynthesis and photo-acclimation: accumulation and mobilisation of energy reserves in phytoplankton. *Marine Ecology Progress Series*, 383, 53–71.

Sciandra, A. and Ramani, P. (1994). The limitations of continuous cultures with low rates of medium renewal per cell. *J. Exp. Mar. Biol. Ecol.*, 178, 1–15.

Sukenik, A. and Livne, A. (1991). Variations in Lipid and Fatty Acid Content in Relation to Acetyl CoA Carboxylase in the Marine Prymnesiophyte *Isochrysis galbana*. *Plant Cell Physiol.*, 32, 371–378.

Thompson-Jr, G.A. (1996). Lipids and membrane function in green algae. *Biochim Biophys Acta*, 1302, 17–45.

Appendix A. COMPUTATION OF FINAL LIPID QUOTA AFTER NITROGEN STARVATION

The dynamics of q_n and q_l, once external nitrate have been exhausted are:

$$\begin{cases} \dot{q_n} = -\mu(q_n)q_n \\ \dot{q_l} = (\beta q_n - q_l)\mu(q_n) \end{cases} \tag{A.1}$$

Using these equations, the dynamic of $v = \frac{q_l}{q_n}$ is:

$$\dot{v} = \frac{q_n\dot{q_l} - q_l\dot{q_n}}{{q_n}^2} = -\frac{\beta}{q_n}\dot{q_n} \tag{A.2}$$

Integrating from t_1 to t_2, we obtain:

$$v_2 - v_1 = \int_{t_1}^{t_2} \dot{v}dt = \int_{q_{n1}}^{q_{n2}} -\frac{\beta}{q_n}dq = [-\beta \ln q_n]_{q_{n1}}^{q_{n2}} \tag{A.3}$$

Now consider a complete starvation from a non limited equilibrium, *i.e.* $q_{n1} = Q_m$, $q_{l1} = (\beta - \gamma)Q_m$, $q_{n2} = Q_0$ and $q_{l2} = q_l^\dagger$, the last expression becomes:

$$\frac{q_l^\dagger}{Q_0} - \frac{(\beta - \gamma)Q_m}{Q_m} = [-\beta \ln q_n]_{Q_m}^{Q_0} = \beta \ln \frac{Q_m}{Q_0} \tag{A.4}$$

From this equation, we can deduce the expression of $q_l^\dagger$.